Delft University of Technology

Document Version
Final published version

Licence
Dutch Copyright Act (Article 25fa)

Citation (APA)
Arslan, O., Messali, F., Smyrou, E., E. Bal, İ., & G. Rots, J. (2024). *Experimental Characterisation of Strengthened Timber Joist-Cavity Wall Connections*. Paper presented at 18th World Conference of Earthquake Engineering, Milan, Italy. https://proceedings-wcee.org/view.html?id=22808&conference=18WCEE

Important note
To cite this publication, please use the final published version (if applicable).
Please check the document version above.

Copyright
In case the licence states “Dutch Copyright Act (Article 25fa)”, this publication was made available Green Open Access via the TU Delft Institutional Repository pursuant to Dutch Copyright Act (Article 25fa, the Taverne amendment). This provision does not affect copyright ownership.
Unless copyright is transferred by contract or statute, it remains with the copyright holder.

Sharing and reuse
Other than for strictly personal use, it is not permitted to download, forward or distribute the text or part of it, without the consent of the author(s) and/or copyright holder(s), unless the work is under an open content license such as Creative Commons.

Takedown policy
Please contact us and provide details if you believe this document breaches copyrights.
We will remove access to the work immediately and investigate your claim.

This work is downloaded from Delft University of Technology.

18TH WORLD CONFERENCE ON EARTHQUAKE ENGINEERING
WCEE2024
MILAN

MILAN, ITALY
30TH JUNE - 5TH JULY 2024
www.wcee2024.it

EXPERIMENTAL CHARACTERISATION OF STRENGTHENED TIMBER JOIST-CAVITY WALL CONNECTIONS

O. Arslan[1&2], F. Messali[3], E. Smyrou[4], İ. E. Bal[5] & J. G. Rots[6]

[1] Researcher, Research Centre for Built Environment NoorderRuimte, Hanze University of Applied Sciences, Groningen, the Netherlands, o.arslan@pl.hanze.nl

[2] Ph.D. Candidate, Faculty of Civil Engineering and Geosciences, Delft University of Technology, Delft, the Netherlands

[3] Researcher/Lecturer, Faculty of Civil Engineering and Geosciences, Delft University of Technology, Delft, the Netherlands

[4] Associate Professor, Research Centre for Built Environment NoorderRuimte, Hanze University of Applied Sciences, Groningen, the Netherlands

[5] Professor, Research Centre for Built Environment NoorderRuimte, Hanze University of Applied Sciences, Groningen, the Netherlands

[6] Professor, Faculty of Civil Engineering and Geosciences, Delft University of Technology, Delft, the Netherlands

Abstract: *Post-earthquake structural damage shows that out-of-plane wall collapse is one of the most common failure mechanisms in unreinforced masonry (URM) buildings. This also represents a critical issue in Groningen, a province located in the northern part of the Netherlands, where man-induced earthquakes have become a significant problem in recent years. Out-of-plane (OOP) failure mechanisms in brick masonry structures often stem from poor wall-to-wall, wall-to-floor or wall-to-roof connections that provide insufficient restraint and boundary conditions. Therefore, studying the mechanical behaviour of such connections is of prime importance for understanding and preventing damages and collapses in URM structures. This paper is about an experimental campaign conducted in the laboratory of the Hanze University of Applied Sciences to characterise the seismic behaviour of strengthened timber joist-masonry cavity wall connections. A total of seven URM wallets were tested, with varying strengthening configurations. Special attention is devoted to the identification of failure mechanisms and hysteretic behaviour for each group of tests performed. The experimental results showed the importance of cohesion and friction between joist and masonry, as the type of failure mechanism (sliding of the joist or rocking failure of the masonry wallet) depends on the value of these two parameters. Additionally, the interaction between the joist and the wallet activated due to rocking led to an arching effect that determined additional friction at the interface between the joist and the masonry and, therefore, increased the force capacity of the connection.*

1. Introduction

Post-earthquake structural observations such as those conducted after the 1997 Umbria-Marche earthquake in Italy (Blasi et al., 1999), the 2009 L'Aquila earthquake in Italy (D'Ayala & Paganoni, 2011), the 2011

Canterbury earthquake in New Zealand (Moon et al., 2014) or the 2015 Gorkha earthquakes in Nepal (Dizhur et al., 2016) show that out-of-plane (OOP) wall collapse is one of the most common failure mechanisms in unreinforced masonry (URM) structures. This is expected to be a critical issue also in Groningen, a province located in the northern part of the Netherlands, where low-intensity man-induced earthquakes have occurred since 1991 due to gas extraction (van Eck et al., 2006).

The building stock in Groningen is commonly constituted by either single-wythe or double-wythe calcium-silicate and clay brick URM walls, timber floor and lack of any specific seismic detailing such as connections between structural elements. Satisfactory seismic performance is achieved when the building vibrates like a monolithic box (Lourenço et al., 2011). To this end, building components need to be well connected since OOP failure mechanisms in brick masonry structures primarily originated from insufficient connections. Therefore, the study of the mechanical behaviour of such connections is of prime importance to understand and prevent damage and collapse in URM structures. Until now, little research has been carried out to characterise the seismic behaviour of wall-to-floor connections, particularly in strengthened conditions, in typical Groningen houses.

In order to understand the dynamic behaviour of URM buildings with flexible diaphragms and evaluate possible strengthening solutions, an experimental campaign on two full-scale two-storey buildings was carried out at the EUCENTRE laboratory in Pavia (Magenes et al., 2014). The structures consisted of timber floors and roofs. The first structure was representative of a vulnerable building lacking connections between walls and floor (Magenes et al., 2010), with the timber joists simply placed on half the width of the external walls. The specimen showed a response characterised by a local out-of-plane failure due to the poor connections. In Building 2, the floor-to-wall connections were improved by the inclusion of anchors. The strengthened building showed a box-type behaviour, preventing premature OOP failures. As a consequence, the strengthened connections significantly increased the seismic performance of Building 2 compared to the first unstrengthened reference prototype.

An extensive multiscale testing was carried out to investigate the seismic behaviour of Dutch houses at EUCENTRE laboratories in Pavia (Graziotti et al., 2019). Full-scale shaking table tests were conducted on a cavity wall terraced house (Miglietta et al., 2019) and a double-wythe clay-brick detached house (Kallioras et al., 2018). The tests showed that although the connections were damaged, no sliding or significant differential displacements between walls and floors were recorded. However, further investigation was necessary to evaluate the performance of individual connections since the focus of the research was based on the global dynamic behaviour of the buildings.

Ravenshorst and Mirra (Mirra & Ravenshorst, 2019) conducted an experimental investigation on different timber joist-masonry wall connections in both as-built and strengthened conditions based on construction practices from the Netherlands, particularly Groningen. The study aimed to evaluate the response of wallets under dynamic loading. A total of seven configurations were studied, of which five configurations represented strengthened conditions. It was reported that the strengthened specimens, compared to the as-built condition, showed increased strength, stiffness, and ductility.

Considering the experimental study already described in the literature, more information on the seismic behaviour of the timber-joist cavity-wall connections must be provided. In order to fill these gaps, an experimental campaign has been carried out at the Hanze University of Applied Science to provide a comprehensive characterisation of the axial behaviour of strengthened timber-joist connections in cavity walls. Section 2 describes the sample geometry, the test setup, and the adopted testing protocol. Section 3 presents the test results with special attention to the developed failure mechanism and the definition of force-displacement curves for each group of tests performed.

2. Test programme and methodology

2.1. Test Specimens

All wallets were constructed on a steel beam by an experienced mason to ensure the best possible quality control. The specimens were built in the laboratory of the Hanze University of Applied Sciences, at BuildinG. The specimens consisted of timber joists pocketed into masonry wallets. The specimens were left to cure for at least 28 days prior to testing (reference specimens) or strengthening (strengthened conditions).

A total of seven wallets were tested in which two specimens represented reference unstrengthened configuration, and five specimens were tested in strengthened condition (Table 1). In common Dutch practice, a cavity wall often consisted of an inner load-bearing leaf and an outer non-loadbearing leaf with an 80mm cavity. In the specimens, the inner leaf was 1030 mm high, 930 mm wide, and 102 mm thick, while the outer leaf was 950 mm high, 930 mm wide, and 100 mm thick (Figure 1a). A timber joist with a size of 55x155 mm and a total length of 1600mm is placed in the calcium silicate (CS) leaf. L-shaped ties with a diameter of 3.6mm are embedded between two bricks in the mortar joint. In the reference specimens, the timber joist end was simply inserted in the inner leaf without any specific connection, representing simple masonry pocket connection (F1 and F2).

Table 1. Overview of the specimens in terms of applied pre-compression level and connections details.

Specimen Name	**Initial pre-comp. level**	**As-built condition**		**Strengthened condition**	
		Timber joist-wall connection	**Number of As-built wall ties**	**Timber joist-wall connection**	**Number of post-installed ties**
F1	0.1 MPa	Pocket connection	2 ties	-	-
F2	0.1 MPa	Pocket connection	2 ties	-	-
F3	0.1 MPa	Pocket connection	2 ties	Timber blocks	-
F5	0.1 MPa	Pocket connection	-	Timber blocks	4 cavity anchors
F6	0.1 MPa	Pocket connection	-	Timber blocks	4 cavity anchors
F7	0.1 MPa	Pocket connection	2 ties	Timber blocks	2 cavity anchors
F8	0.1 MPa	Pocket connection	2 ties	Timber blocks	2 cavity anchors

Regarding the strengthened connections, three different configurations were considered: (i) one wall was retrofitted using timber blocks (F3), (ii) two walls without as-built wall ties were retrofitted using the timber blocks and post-installed cavity wall tie anchors (F5 and F6), (ii) two walls with as-built cavity-wall ties were retrofitted using the timber blocks and post-installed cavity wall tie anchors (F7 and F8). A summary of geometrical details and boundary conditions of Specimens F7 and F8 is presented in Figure 1b.

The installation overview of the timber blocks and post-installed mechanical anchors is shown in Figure 1c and d. Timber blocks with mechanical anchors were used to strengthen the connection between the timber joist and the inner leaf of the cavity wall. The timber blocks were placed on both sides of the joist and fastened to the inner leaf by means of anchors with a total length of 120 mm and a diameter of 10 mm and then screwed to the joist with steel angles (Figure 1c).

The post-installed cavity wall tie anchors were used to strengthen the connection between two leaves of the cavity wall. 225 mm long cavity anchors with 8 mm diameter were inserted through bricks. The first step consisted of pre-drilling through the brick face of the inner leaf until almost the middle of the outer leaf. Then, the tie anchor and its plug were placed into the pre-drilled hole, as shown in Figure 1d.

For Specimen F5 and F6, which lack as-built ties, a total of four post-installed cavity anchors were placed at the 5th and 10th courses from the bottom of the inner leaf. Regarding Specimen F7 and F8, only two post-installed cavity anchors were located at the 10th course from the bottom of the inner leaf.

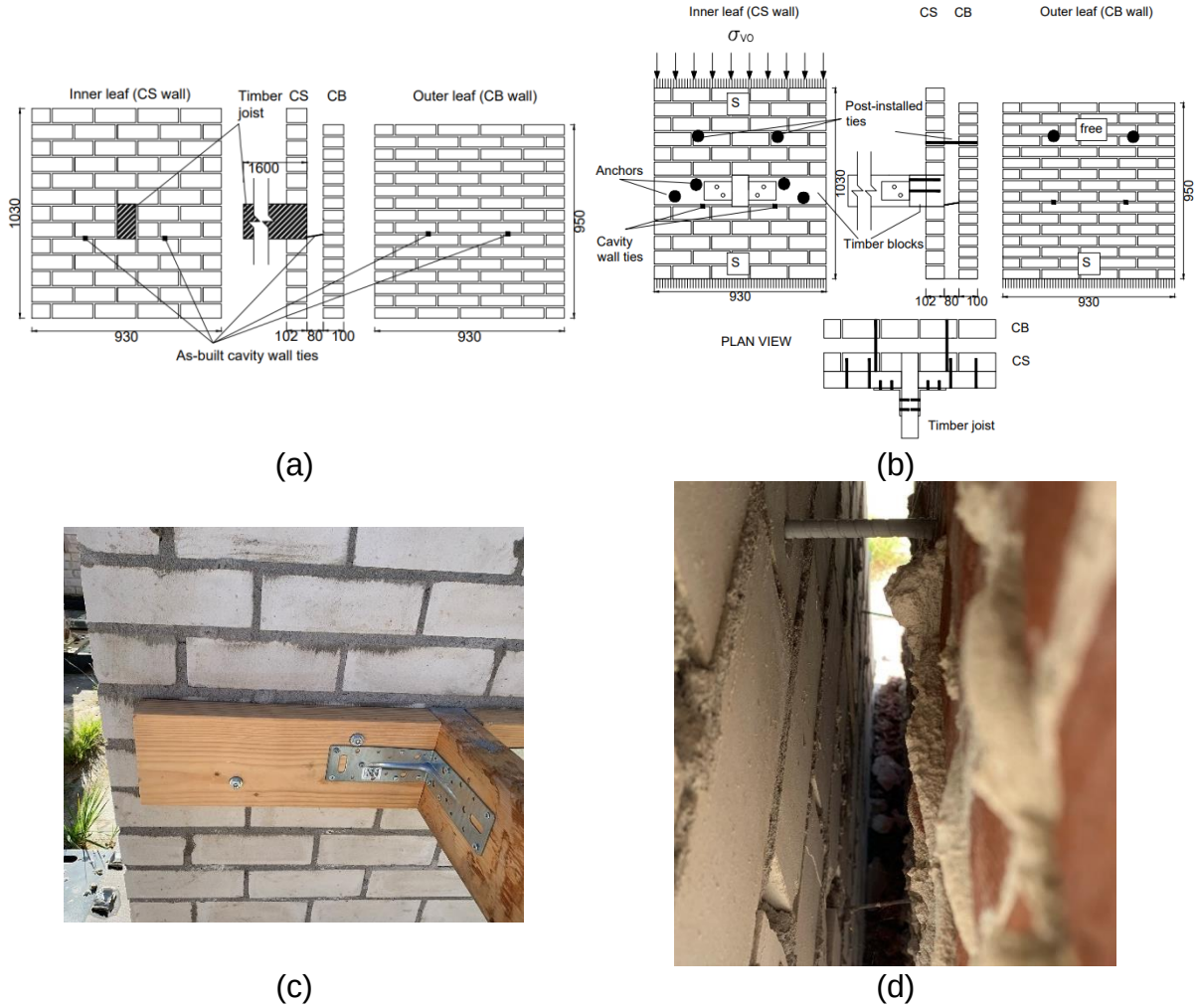

Figure 1. Overview of the wallets: geometry of the reference specimens (a) and the strengthened connections (b), installing procedure for anchors used in timber blocks with steel angle between timber joist and block (c), and post-installed cavity wall anchors (d).

2.2. Test setup

The specimens were tested on an out-of-plane setup at the BuildinG laboratory. The test setup consisted of a reaction frame, two air bellows, and an actuator. The reaction frame had a width of 2250 mm, a depth of 2250 mm, and a height of 1900 mm. A bottom steel plate was used to restrain the specimen to the frame, and the specimens were built on the steel beam. The specimens were subjected to vertical precompression via two air bellows to simulate the effect of load-bearing walls acting on the cavity wall (Figure 2a). A vertical dead load of 100kg was applied to the middle of the joist to simulate the self-weight of the floor portion supported by the joist.

The specimens were loaded via the joist with an electric actuator. The actuator is capable of tension/compression of 30 kN, integrated with a data acquisition system. The actuator was positioned over the joist and aligned horizontally along the joist's centreline axis. The free end of the joist was connected to the actuator, allowing for the transfer of the applied load in the uniaxial direction of the joist through the pressure apparatus (Figure 2b). Potentiometers were used to measure the absolute displacement of the inner and outer leaves, while LVDTs were used to obtain the relative displacement between the CS leaf and joist.

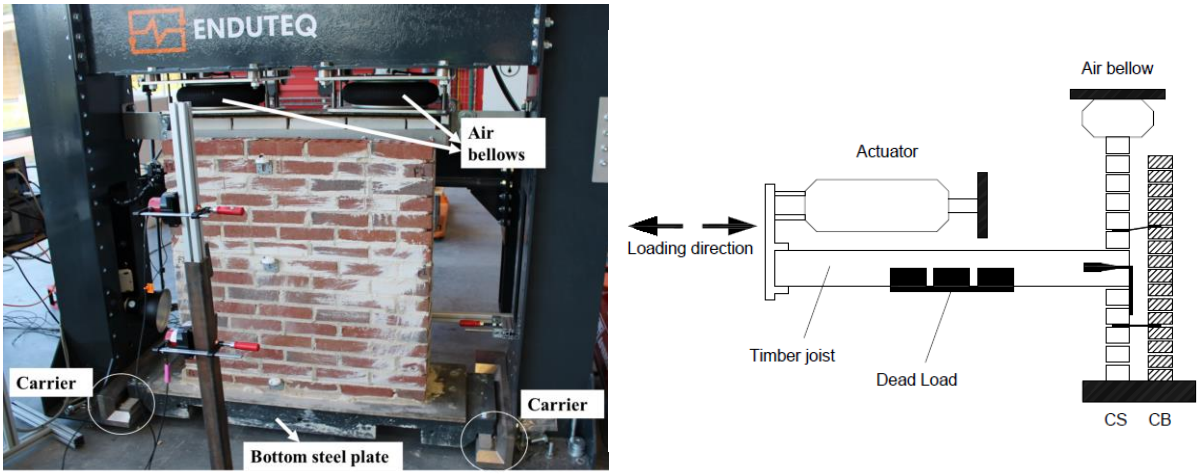

(a) (b)

Figure 2. Overview (a) and schematic view (b) of the test setup.

2.3. Loading protocols

The specimens were subjected to a quasi-static reversed-cyclic test based on Method B of the ASTM standard (2019), initially developed for ISO 16670 (2003). A displacement-controlled procedure was used during the test. A monotonic test was conducted by Mirra (2019) to determine the ultimate displacement for the reference deformation of the test. Therefore, the reference deformation of the cyclic test in this study was derived from the monotonic test conducted by Mirra (2019). The loading protocol consisted of three fully reserved cycles with a displacement ranging from 1.25% to 280%. The loading rate was set at three mm/s.

3. Test results

3.1. Hysteretic behaviour

Force-displacement curves were generated, as presented in Figure 3. The relative displacement between the joist and wall is indicated on the horizontal axis of Figure 3. No significant difference between the as-built and strengthened conditions was observed since additional contributions due to vertical forces caused by arching actions within the walls were observed, as discussed in detail in the following section. However, the main difference between the reference specimens and the strengthening method was that during the experiment, there was a progressive shift towards only one side of loading, specifically the pulling (positive) direction, in which slippage developed due to the pull-out of the anchors from the wallet. On the other side, while pushing the joist towards the wallets, the slippage of the joist remained in the same position. It should be noted that despite being a strengthened specimen with timber blocks, Specimen F3 exhibited symmetrical behaviour for both loading directions due to retrofitting only using the timber blocks lacking post-installed cavity wall tie anchors, leading to lower OOP capacity of the wallet, which caused it to exhibit rocking behaviour.

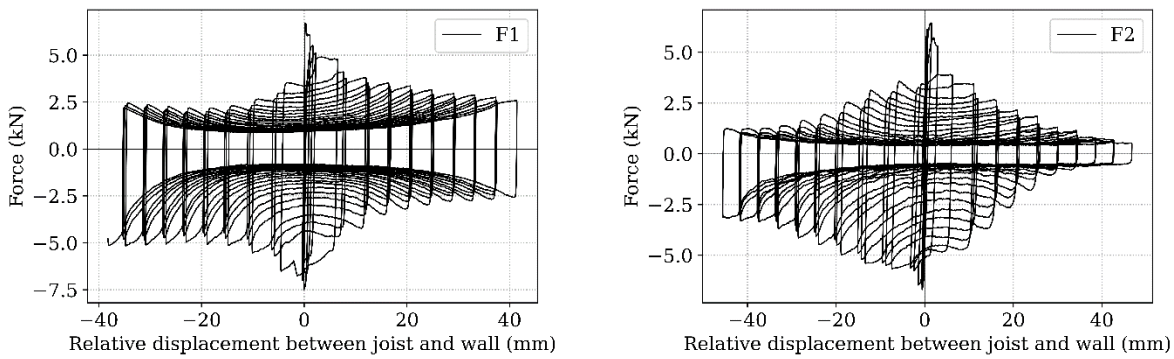

(a) (b)

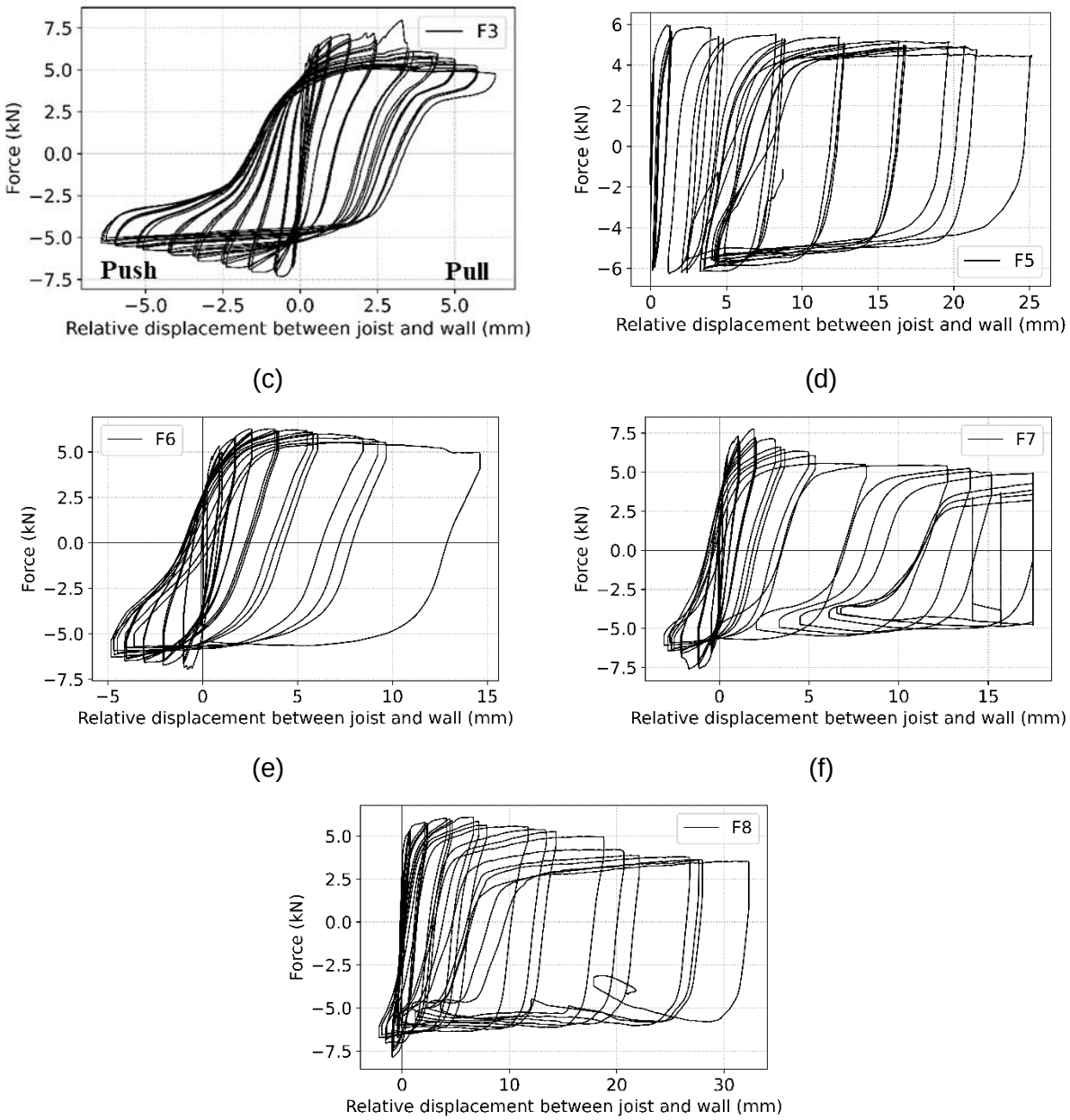

Figure 3. Hysteresis curves of the unstrengthened specimens.

Specimen F3 (the specimen retrofitted using timber blocks) exhibited the highest strength capacity in pulling. The hysteresis curve was quite symmetrical, indicating similar behaviour for both loading directions. In pulling, an initial linear elastic behaviour of the connection up to about half of the peak load was followed by hardening up to the peak. The post-peak phase was characterised by softening.

Specimens F5 and F6 had the same configuration. The hysteresis curves of F5 and F6 were unsymmetrical, presenting a similar behaviour. An initial linear elastic behaviour of the connection up to about one-sixth of the peak load was followed by hardening up to the peak. The post-peak phase was characterised by softening.

Although Specimens F7 and F8 with as-built cavity-wall ties were retrofitted using post-installed cavity wall tie anchors and Specimens F5 and F6 without as-built cavity-wall ties were retrofitted using post-installed cavity wall tie anchors, the capacity of Specimens F7 and F8 were of a similar magnitude to the peak forces from Specimens F5 and F6. As the total number of ties was the same for all the specimens mentioned above, the specimens only with post-installed cavity wall tie anchors would exhibit a higher capacity since they have a higher strength capacity.

3.2. Mechanical contribution to the total connection resistance

As noted in the previous section, additional vertical forces were introduced at the joist-wallet interface determined by the boundary conditions of the test setup in which the air bellows partially restrained the vertical displacement at the top of the inner leaf. The way the vertical load was applied led to activating an arching effect after starting the rocking failure mode. The arching effect determined increased compressive stress on the contact area between the joist and the masonry with increasing horizontal displacement of the inner leaf. Therefore, the frictional resistance increased gradually at the increase of the OOP displacements of the inner leaf.

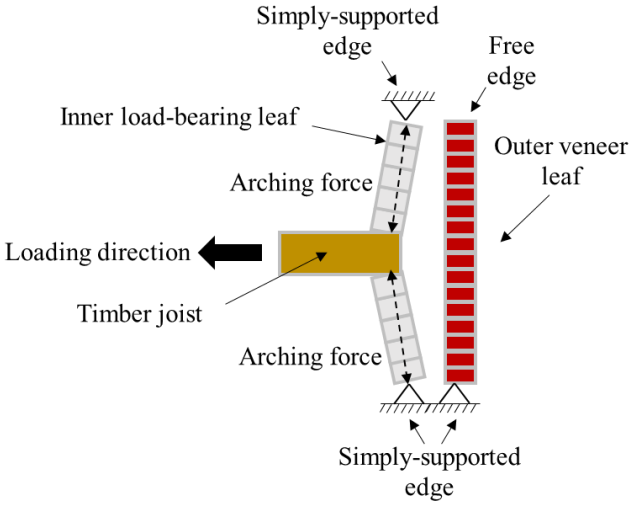

Figure 4. Schematic description of the arching effect mechanism.

3.3. Failure mechanism

The reference specimens (F1 and F2) exhibited a joist-sliding failure mode, while the strengthened specimens (F3, F5, F6, F7 and F8) exhibited a rocking failure mode. The former failure mode was characterised by the joist sliding, which includes partial joist-to-wall interaction. The joist-sliding failure mode depended on cohesion and friction between joist and masonry, as well as by the arch effect activated due to the joist-to-wall interaction. In addition, diagonal cracks propagating from the joist were observed. The latter failure mode was characterised by the rocking behaviour of both leaves of the wall.

Regarding the strengthened specimens, except for Specimen F3, a local failure mechanism at the anchors between the wallet and the timber blocks occurred in addition to the rocking failure mode. The specimens presented a failure of the connection between the timber blocks and the inner leaf due to the presence of post anchors sufficiently increased OOP capacity shifting than the weakest failure mechanism from rocking to the failure of the connection. On the other side, regarding Specimen 3 lacking post-installed cavity wall tie anchors, the inner leaf was not restrained to horizontal displacement via the cavity wall tie anchors; hence, the OOP capacity of the wallet was weaker than the capacity of the connections between the timber block and the wallet, exhibiting rocking behaviour.

The deformed shape of strengthened specimens with maximum displacement in positive and negative directions can be seen in Figure 5. The inner and outer leaves undergo the rocking type behaviour, resulting in the formation of a hinge at the bottom and middle height of the CS leaf. Hence, the rocking behaviour was the governing failure mode.

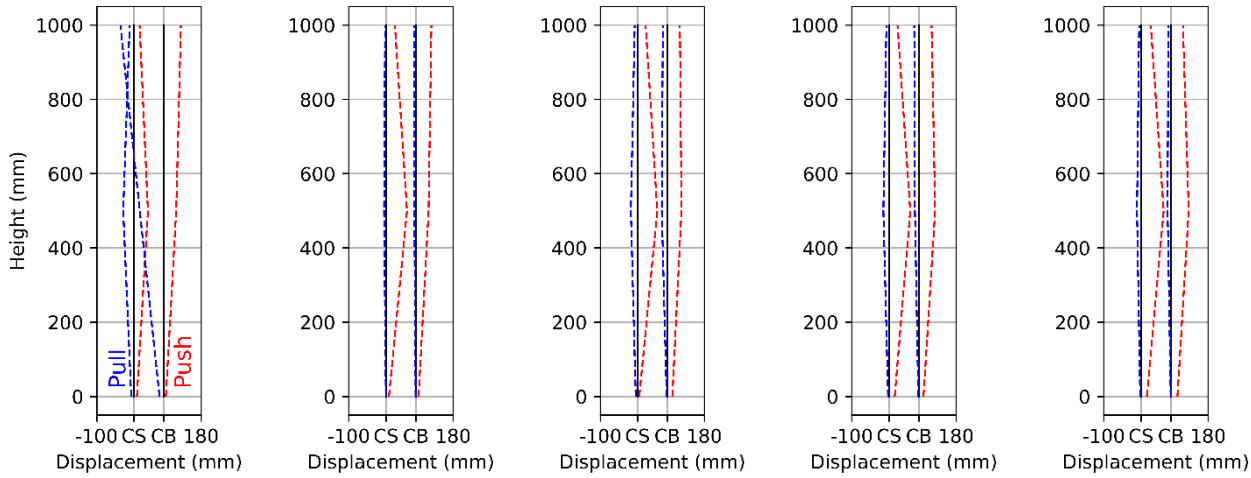

(a) F3 (b) F5 (c) F6 (d) F7 (e) F8

Figure 5. Deformed shapes of the strengthened specimens. The dashed lines indicate envelope deformed shapes in positive and negative directions.

4. Conclusions

The paper presents the results of an experimental campaign that consists of quasi-static cyclic tests performed on strengthened timber-joist cavity-wall specimens. The paper aims to provide a comprehensive characterisation of the behaviour of the timber-joist cavity-wall connections under axial cyclic loading.

Two different failure modes were obtained: joist-sliding and rocking failure modes. In the case of the reference specimens exhibiting the joist-sliding failure mode, the failure mode was characterised by the cohesion and friction between the joist and masonry. Hence, the diagonal cracks propagating from the joist in the shape of punching shear were due to the bonding between the joist and the masonry wall. Additionally, the capacity of the connection was affected by an additional vertical force due to the arching effect. This force, resulting from the arching effect, increased with larger horizontal displacements, leading to a higher frictional force at the interface between the joist and masonry.

In the case of the strengthened connections exhibiting the rocking failure mode, the failure was attributed to the rocking of the wallet. Therefore, the capacity was primarily governed by the out-of-plane behaviour of the cavity wall system. This behaviour was influenced by the flexural strength of both the inner and outer leaves and the coupling force provided by the ties between the leaves. In general, only a slight increase in capacity compared to the as-built condition was observed for the strengthened specimens, as an OOP rocking mechanism was already activated for the as-built condition. This limits the capacity of the wall system so that the improvement of the connection performance has little influence.

5. References

Blasi, C., Borri, A., Di Pasquale, S., Malesani, P., Nigro, G., Parducci, A., & Tampone, G. (1999). *Manuale per la riabilitazione e la ricostruzione sismica degli edifici — Regione dell'Umbria*. DEI Tipografia del Genio Civile.

D'Ayala, D. F., & Paganoni, S. (2011). Assessment and analysis of damage in L'Aquila historic city centre after 6th April 2009. *Bulletin of Earthquake Engineering*, *9*(1), 81–104. https://doi.org/10.1007/s10518-010-9224-4

Dizhur, D. Y., Dhakal, R. P., Bothara, J., & Ingham, J. M. (2016). Building typologies and failure modes observed in the 2015 Gorkha (Nepal) earthquake. *Bulletin of the New Zealand Society for Earthquake Engineering*, *49*(2), 211–232. https://doi.org/10.5459/bnzsee.49.2.211-232

Graziotti, F., Penna, A., & Magenes, G. (2019). A comprehensive in situ and laboratory testing programme supporting seismic risk analysis of URM buildings subjected to induced earthquakes. *Bulletin of Earthquake Engineering*, *17*(8), 4575–4599. https://doi.org/10.1007/s10518-018-0478-6

Kallioras, S., Guerrini, G., Tomassetti, U., Marchesi, B., Penna, A., Graziotti, F., & Magenes, G. (2018). Experimental seismic performance of a full-scale unreinforced clay-masonry building with flexible

timber diaphragms. *Engineering Structures*, *161*(February), 231–249. https://doi.org/10.1016/j.engstruct.2018.02.016

Lourenço, P. B., Mendes, N., Ramos, L. F., & Oliveira, D. V. (2011). Analysis of Masonry Structures Without Box Behavior. *International Journal of Architectural Heritage*, *5*(4–5), 369–382. https://doi.org/10.1080/15583058.2010.528824

Magenes, G., Penna, A., & Galasco, A. (2010). A full-scale shaking table test on a two-storey stone masonry building. *14th European Conference on Earthquake Engineering*, *August*, 384.

Magenes, G., Penna, A., Senaldi, I. E., Rota, M., & Galasco, A. (2014). Shaking Table Test of a Strengthened Full-Scale Stone Masonry Building with Flexible Diaphragms. *International Journal of Architectural Heritage*, *8*(3), 349–375. https://doi.org/10.1080/15583058.2013.826299

Miglietta, M., Mazzella, L., Grottoli, L., Guerrini, G., & Graziotti, F. (2019). Full-scale shaking table test on a Dutch URM cavity-wall terraced-house end unit – EUC-BUILD-6. *Research Report EUC160/2018U*.

Mirra, M., & Ravenshorst, G. J. P. (2019). *Seismic characterization of timber-masonry connections based on experimental results*.

Moon, L., Dizhur, D. Y., Senaldi, I., Derakhshan, H., Griffith, M. C., Magenes, G., & Ingham, J. M. (2014). The Demise of the URM Building Stock in Christchurch during the 2010–2011 Canterbury Earthquake Sequence. *Earthquake Spectra*, *30*(1), 253–276. https://doi.org/10.1193/022113EQS044M

van Eck, T., Goutbeek, F., Haak, H., & Dost, B. (2006). Seismic hazard due to small-magnitude, shallow-source, induced earthquakes in The Netherlands. *Engineering Geology*, *87*(1–2), 105–121. https://doi.org/10.1016/j.enggeo.2006.06.005